Protection of Transmission Lines Using Global Positioning Systems (GPS)

R.O. Okeke & M. Ehikhamenle
Department of Electronic and Computer Engineering,
University of Port Harcourt, Choba, Rivers State,
Nigeria
remyokeke@yahoo.co.uk mattinite4u@yahoo.com

Abstract
In this research, protection of transmission lines using Global Positioning Systems (GPS) is presented. The proposed idea has the feature of unit protection relays to protect large power transmission grids based on phasor measurement units. The principle of the protection scheme depends on comparing positive sequence voltage magnitudes at each bus during fault conditions inside a system protection center to detect the nearest bus to the fault. Then the absolute differences of positive sequence current angles are compared for all lines connecting to this bus to detect the faulted line. The new technique depends on synchronized phasor measuring technology with high speed communication system and time transfer GPS system. The simulation of the interconnecting system is applied using Matlab Simulink. The new technique can successfully distinguish between internal and external faults for interconnected lines. The new protection scheme works as unit protection system for long transmission lines. The time of fault detection is estimated by 0.00345 m/sec for all fault conditions and the relay is evaluated as a backup relay based on the communication speed for data transferring.

Keyword*; GPS System, Matlab Simulink, Transmission Grids*

1. INTRODUCTION

System-wide disturbances in power systems are a challenging problem for the utility industry because of the large scale and the complexity of the power system. When a major power system disturbance occurs the protection and control actions are required to stop the power system degradation, restore the system to a normal state, and minimize the impact of the disturbance (Novosel *et al.,* 1995). The present control actions are not designed for a fast developing disturbance and may be too slow. Further, dynamic simulation software is applicable only for off-line analysis.

The recent enlargement and increased complexity of power system configurations has led to adjacent arrangements of short and long distance power transmission lines, both connected to the same busbar in a substation (Brahma, 2005). This causes difficult situations when relay engineers coordinate reach or operate time among distance relays. To cope with this, current differential protection which utilizes wide-area current data would be effective for wide-area backup protection although such protection needs system-wide timing synchronism for the simultaneous current sampling at all remote terminals and data exchanges among them. The on-going reforms in the Nigerian power sector incorporate among its numerous objectives, to produce radical expansion of the existing grid network. It is expected that in the next few years, a much superior, fortified and secure grid will replace the inadequate, unstable and delicate grid in Nigeria (Balogun, 2007). The rapid increase in the demand for electricity as a

result of population growth, industrial development and rise in consumer electrical appliances have necessitated the stepping up of generation and transmission capabilities of the grid network to deliver quality power supply to the consumers. It becomes therefore necessary to fulfill the requirement of load without any fault in providing bulk power from sending end to receiving end in short duration of time. At such, there is need to effectively detect and manage the associated faults inevitable in all transmission lines. Faults detection on transmission lines using conventional means can be very costly and inconclusive. In power transmission systems, accurate location of faults will not only save time but helps to optimally utilize resources available for electricity supply. Thus, power system operator needs accurate information transferred speedily in a form most suitable to communicate with field personnel.

2.LITERATURE REVIEW

In electrical utilities, transmission lines form the backbone of power systems. With regard to reliability and maintenance costs of power delivery, accurate fault location for transmission lines is of vital importance in restoring power service, and reducing outage time as much as possible. Many fault location techniques have been proposed in open literature (Yang, 2008). Among these techniques, specifically (Takagi et al., 1981) applied the superposition principle to estimate single-ended fault location algorithms. The said authors' approaches were very attractive as they did not require communication to obtain results. However, algorithms based on single ended data will affect accuracy due to variations in source impedances, fault incidence angle, fault impedance, and loading conditions. With the advent of global positioning system (GPS)-based synchronously measuring units including phasor measurement units (PMUs) (Phadke and Thorp, 2008), digital relays, and digital fault recorders in the early 1990s, GPS-based fault location techniques (Kezunovic, 1994) have become promising. The main advantage of GPS-based techniques is that fault location estimation accuracy is unaffected by variations in source impedances and fault impedances due to the availability of two-terminal synchronized data.

Kezunovc *et al. (*1996) employed synchronized voltages and currents samples at two terminals to estimate the fault location. They adopted a time-domain model as basis for the algorithm development. However, data must be acquired at a sufficiently high sampling rate to provide adequate approximation of the derivatives.

For their part, (Lee et al.2006) utilized synchronized phasors at both terminals to obtain the fault location. Their algorithm was based on positive and zero sequence components of post fault voltages and currents. In particular, errors will be presented when dealing with three-phase faults where zero sequence components are absent. Moreover, their work only considered a short line model that could not reflect the nature of transmission lines. Meanwhile, our previous works (Lin *et al.,* 2004) proposed fault location/detection techniques for transmission lines using synchronized phasor measurements. The developed fault location/detection indices can be used for transmission line protection as well (Chen *et al.,* 2012). However, due to the high installation cost of PMUs, majority of utilities install PMUs only at key substations. Thus, the digital measurements at two line terminals are acquired asynchronously in the absence of GPS signal. Therefore, fault location estimation based on two-terminal data will suffer in terms of accuracy. Consequently, fault locations based on post fault data synchronization algorithms were considered in some papers. Girgis *et al.* (1992) used an iterative method to achieve time synchronization.

The fault location method proposed by Dalcastagnê *et al. (*2008) was based on voltage magnitudes. The proposed work (Yu, 2010) used the imaginary part of the fault location index to synchronize the measurements. To achieve a compromise between construction cost

and environmental protection in Taiwan, overhead lines combined with underground cables have been widely adopted by the Taiwan Power Company (Taipower) with 161 kV and 345 kV transmission systems. However, the developed techniques cannot locate the fault accurately using these kinds of compound lines. Thus, a two-terminal multisection line model must be considered to develop a new fault location method.

Gilany *et al. (*2005) used synchronized measurements to detect/locate a fault for a two-section line combined an overhead line with an underground power cable section. Their work required identifying the fault type before locating a fault. Meanwhile, their method is applicable only to two-section compound transmission lines instead of more general multisection compound lines.

2.2 Traveling Wave Fault Location Theory

Traveling wave fault locators make use of the transient signals generated by the fault. When a line fault occurs, such as an insulator flashover or fallen conductor, the abrupt change in voltage at the point of the fault generates a high frequency electromagnetic impulse called the traveling wave which propagates along the line in both directions away from the fault point at speeds close to that of light. The fault location is determined by accurately time-tagging the arrival of the traveling wave at each end of the line and comparing the time difference to the total propagation time of the line.

Unlike impedance-based fault location systems, the traveling wave fault locator is unaffected by load conditions, high ground resistance and most notably, series capacitor banks. This fault locating technique relies on precisely synchronized clocks at the line terminals which can accurately time-tag the arrival of the traveling wave. The propagation velocity of the traveling wave is roughly 300 meters per microsecond which in turn requires the clocks to be synchronized with respect to each other by less than one microsecond.

Precisely synchronized clocks are the key element in the implementation of this fault location technique. The required level of clock accuracy has only recently been available at reasonable cost with the introduction of the Global Positioning System.

The voltage and current at any point x obey the partial differential
Equations

$$\frac{\partial e}{\partial x} = -L\frac{\partial i}{\partial t} \text{ and } \frac{\partial i}{\partial x} = -C\frac{\partial e}{\partial t} \quad \ldots\ldots\ldots\ldots\ldots\ldots\ldots\ldots\ldots 2.1$$

Where L and C are the inductance and capacitance of the line per unit length.

The resistance is assumed to be negligible. The solutions of these equations are;

$$e(x,t) = e_f(x-vt) + e_r(x+vt) \quad i(x,t) = \frac{1}{z}e_f(x-vt) - \frac{1}{z}e_r(x+vt)$$

…….2.2

Where Z = (L/C) is the characteristic impedance of the transmission line and v=1/(LC) is the velocity of propagation. Forward (e_f and i_f) and reverse (e_r and i_r) waves, leave the disturbed area "x" traveling in different directions at "v", which is a little less than the speed of light, toward transmission line ends. Transmission line ends represent a discontinuity or impedance change where some of the wave's energy will reflect back to the disturbance. The remaining energy will travel to other power system elements or transmission lines. Figure 2.5, a Bewley lattice diagram, illustrates the multiple waves (represented by subscripts 2 and 3) generated at line ends. Wave amplitudes are represented by reflection coefficients ka and kb which are

determined by characteristic impedance ratios at the discontinuities. ta and t*b* represent the travel time from the fault to the discontinuity.

With GPS technology, ta and t*b* can be determined very precisely.

By knowing the length (*l*) of the line and the time of arrival difference (ta – t*b*), one can calculate the distance (x) to the fault from substation A by:

$$X = \frac{l - c(\tau_a - \tau_b)}{2} \quad \text{……..2.3}$$

Where c= the wave propagation of 299.79 mm/sec (@ 1ft/ns).

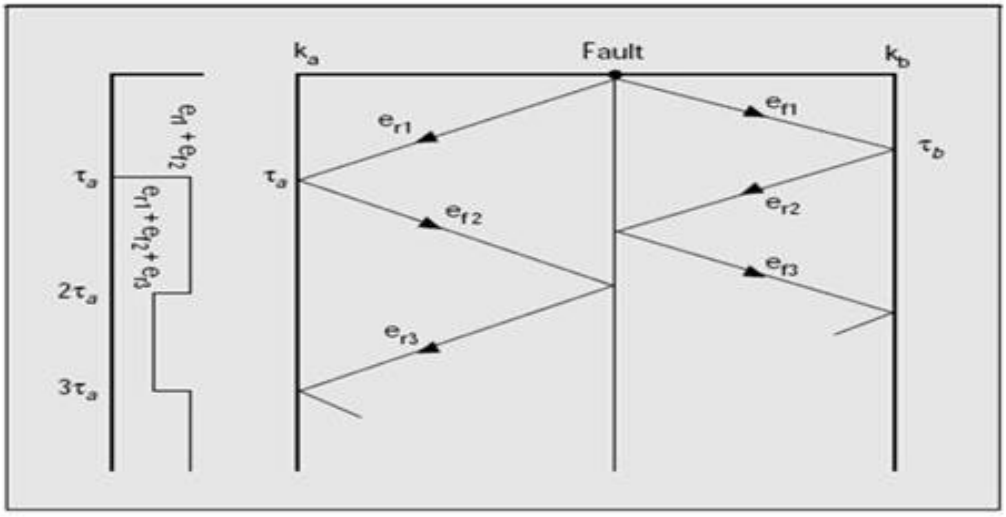

Figure 1: Bewley Lattice Diagram

3. DESIGN METHODOLOGY

The Global Positioning System (GPS) Satellite Circles the earth twice day. It transmits signal into the earth. GPS receivers uses this signal to calculate the users exact location.

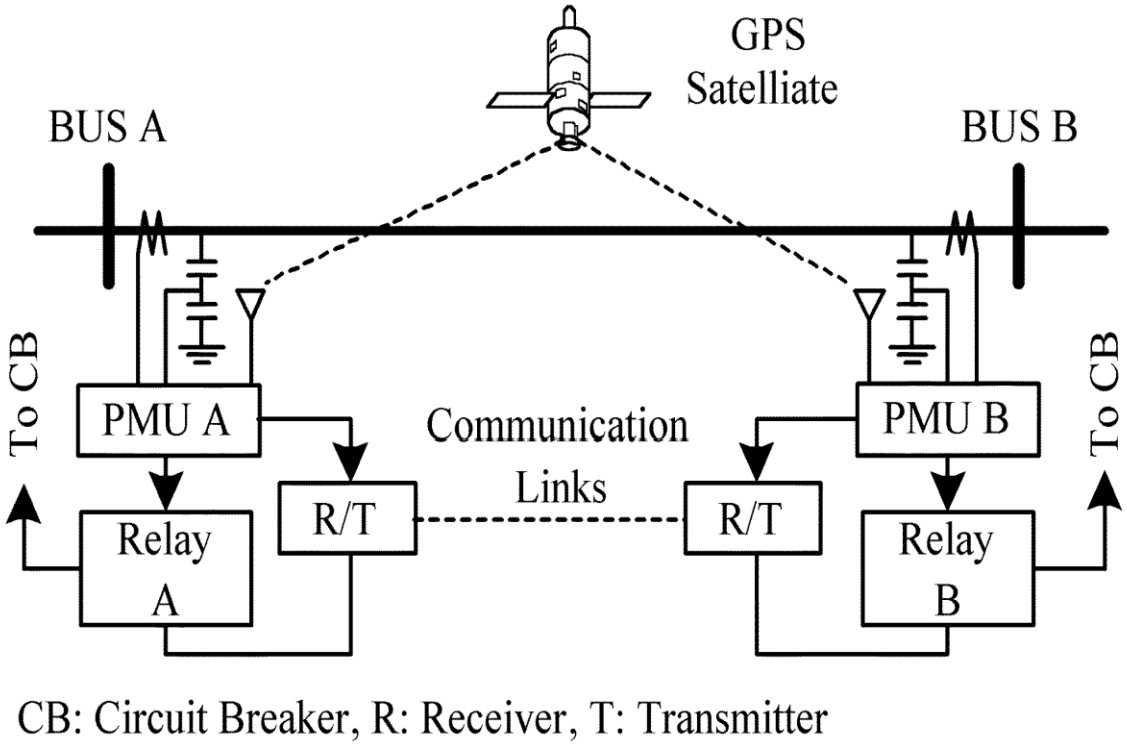

Fig. 2 Block Diagram of the Proposed Protection System.

3.1 Protection System And Algorithm

The proposed protection system is shown in Fig. 3.0 The basic concept and algorithm of the scheme will be described briefly.

A. Data Synchronization

The three-phase phasors of voltage and current are measured simultaneously by PMUs at both ends of line. The global synchronism clock generator (GSCG) [10] has been built in the PMUs to provide an accurate and reliable external reference clock signal. The sampling synchronization of the PMU-GSCG configuration has been verified through field tests of Taipower161-kV substations [10].

B. Communication Links

The synchronized phasors of voltage and current are sent over high-speed communication links to the relays at the other ends of the protected line.

With the rapid development of fiber-optic and digital-communication systems, multiplexed digital channels are often available for use with transmission-line protection. Therefore, high speed for data transfer can be achieved so that the transmission delay can be added only a few milliseconds to the tripping decision time of the protection scheme. Furthermore, the use of redundant communication links can ensure the overall reliability of the protection scheme.

3.2. Fault Location Technique

Fig.3.1 shows a single-circuit transposed transmission line. In Fig.3.1, total line length between buses S and R is assumed to be L, and the synchronized voltage and current phasors measured S and R are Vs, Is, VR and IR, respectively. Using symmetrical components transformation to decouple three-phase quantities (Gross, 1986) and to consider only the variation of a distance variable x (km), the relation between the voltages and currents at a distance x away from bus R can be expressed by the following sequence equations:

$\frac{dV_{012}}{dx} = Z_{012}I_{012}$ ……3.1

$\frac{dI_{012}}{dx} = Y_{012}V_{012}$ ……..3.2

Where Z_{012} and Y_{012} are the per-unit length sequence impedance (Ohm/km) and admittance (Mho/km) of the transmission line, respectively. The matrices of Z_{012} and Y_{012} are all diagonal matrices, and the diagonal entries of matrices Z_{012} and Y_{012} are (Z_0,Z_1,Z_2) and (Y_0,Y_1,Y_2), respectively. Furthermore, $I_{012} = [I_0\ I_2\ I_3]^T$ and $V_{012} = [V_0\ V_2\ V_3]^T$. The variables with the subscripts 0, 1, 2 denote the zero-, positive-, and negative-sequence variables, respectively. The solutions of voltages and currents of the three decoupled sequence systems can be written as (Liao and Kezunovic, 2007).

$Vxi = A_i\exp(r_i\ x) + B_i\exp(-r_i\ x)$ ……..3.3

$Ixi = \frac{1}{z_{ci}}[A_i\exp(r_i\ x) - B_i\exp(-r_i\ x)]$ ……..3..4

where the subscript i denotes 0, 1, and 2 sequence variables, $\frac{1}{z_{ci}} = \sqrt{\frac{Z_i}{Y_i}}$ denotes the characteristic impedance, and $r_i = \sqrt{Z_iY_i}$ is the propagation constant. The constants A_i and B_i can be obtained by the boundary conditions of voltages and currents measured at bus R and bus S respectively. Therefore, voltage (3) can be further rewritten as;

$V_{xi,}R = \frac{V_{i,R} + Z_{Ci}I_{i,R}}{2}e^{r_{ix}} + \frac{V_{i,R} - Z_{Ci}I_{i,R}}{2}e^{-r_{ix}}$ ……3.5

$V_{xi,}S = \frac{1}{2}e^{-r_i}L(V_{i,S} + Z_{Ci,}I_{i,S})e^{r_{ix}} + \frac{1}{2}e^{r_i}L(V_{i,S} - Z_{Ci,}I_{i,S})e^{-r_{ix}}$ ……..3.6

Equations (3.5) and (3.6) represent the voltages at point x, which are expressed in terms of the two data sets (Vi,R, Ii,R) and (Vi,s, Ii,s) measured at the receiving end R and sending end S of the line, respectively. Meanwhile, the positive-sequence quantities can respond to all fault types; thus, they are chosen to determine the fault locations in the current study to avoid fault type identification. For ease of illustration, subscript i=l, which denotes the positive-sequence quantities, is dropped. A fault is assumed to occur at point F with a distance x=DL km away from the receiving end R on a transmission line shown in Fig. 3.1, where D is termed as the per-unit fault location index. Using the relationship VF,R= VF,S and equating (5) to (6), the index can be solved as follows:

$D = \frac{In(\frac{N}{M})}{2rL}$……....3.7

Where

$M = \frac{1}{2}(V_S + Z_C\ I_S)e^{-r_{ix}} - \frac{1}{2}(V_R + Z_C\ I_R)$……3.8

$\frac{1}{2}(V_R - Z_C\ I_R) - \frac{1}{2}(V_{i,S} - Z_C\ I_S)e^{r_L}$ ……..…39

When a fault occurs between buses S and R, the obtained Value D of is between 0 and 1. When no fault or an external fault occurs, the value of D is indefinite. It is worth mentioning that there is no assumption made in the procedure of derivation for the fault location index D. Thus, D the index is unaffected by the variations in source impedance, loading change, fault impedance, fault inception angle, and fault type.

3.2.1Fault Location Technique for Two-Terminal Multi-Section Compound Transmission Lines

Two-Section Compound Lines: First, we consider a two section compound transmission line in which a section of overhead line is connected with the other section of underground power cable, as shown in Fig.3. 2. PMUs or digital relays are assumed to be installed at buses S and R. Therefore, we can acquire two-terminal synchronized voltage and current phasors using GPS technique or fault-on relay data synchronization algorithms.

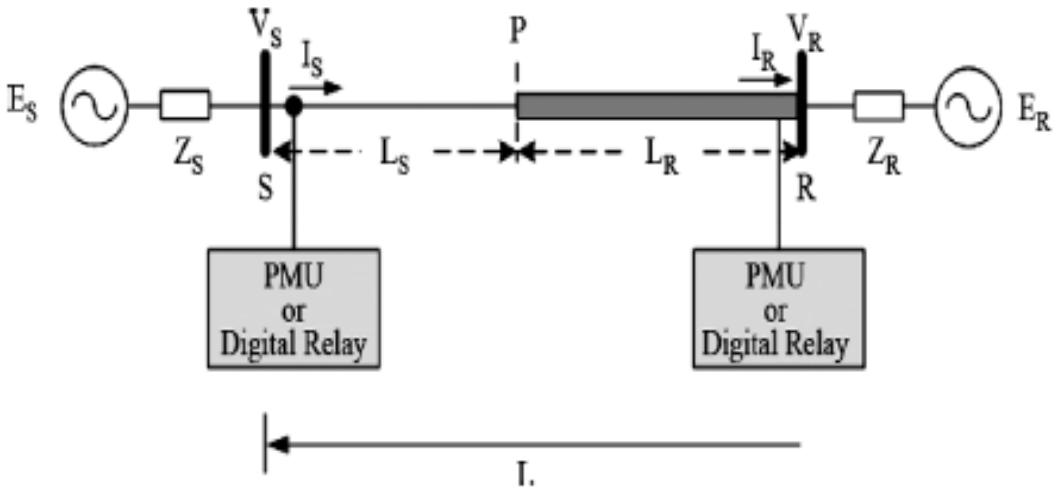

Fig. 3: One line diagram of a two-section compound transmission line; the thin line denotes the overhead line and the bold line denotes the power cable.

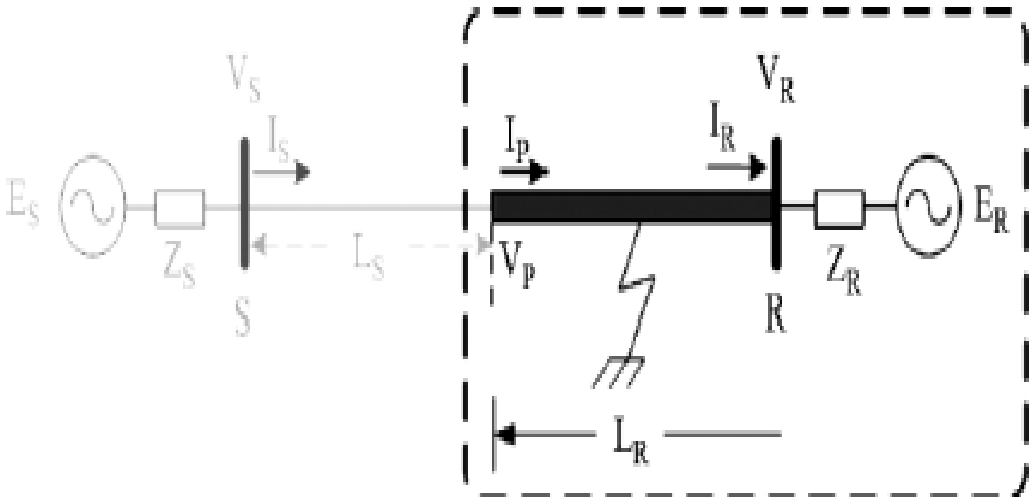

Fig. 4: A fault on the underground power cable section.

Lengths of the overhead line and underground power cable are denoted as Ls and LR , respectively. Total line length between buses S and R is L. Tap point P of the transmission line is selected as the junction point between the LS and LR, which can be defined as the virtual receiving end of the overhead line or the virtual sending end of the cable. A non-uniform line impedance is obtained in this case due to the nature of compound lines. For example, the surge impedance of the cable is approximately 10% of that of an overhead line (Liu, 1982). The proposed fault location technique in this case is expressed using the following steps:

Step 1: ***Assume a fault on the right side of tap point P.*** As shown in Fig. 3, we assume that the fault is situated on the underground power cable LR. Since the healthy section is the overhead line LS , the voltage and current at any point in the overhead line can be derived by applying boundary conditions of bus S into (3) and (4). Consequently, we can obtain the voltage and current phasors at tap point P in terms of the sending end data sets (VS,IS) as

$$V_{p,s} = \frac{1}{2} e^{-\gamma_s} L_s (V_S + Z_C I_S) + \frac{1}{2} e^{\gamma_i} Ls (V_R - Z_{C,s} I_R) \quad \text{.....3.10}$$

$I_{P,S}= \frac{1}{Z_{C,S}} [\frac{1}{2} e^{- r_s} L_s (V_S + Z_{C,S} I_S) - \frac{1}{2} e^{r_i} Ls (V_S - Z_{Ci,} I_S)]$ 3.11

Where $Z_{C,S} = \sqrt{\frac{Z_S}{Y_S}}$ and $r_s = \sqrt{Z_S Y_S}$ denote the characteristic impedance and the propagation constants of the overhead line section, respectively. ZS and YS are the positive sequence impedance and admittance of the LS, respectively. Now we derive the fault location index, using voltage and current phasors at tap point and bus and the line length. Substituting , expressed in (10), (11) into , in (6) and equating (5) to the newly derived (6) with the characteristic impedance, ZC,R and the propagation constant, Γ_R for the power cable section, respectively, the fault location index D1 can be obtained as follows

Di = $\frac{In(\frac{N_R}{M_R})}{2 r_R L_R}$.....3.12

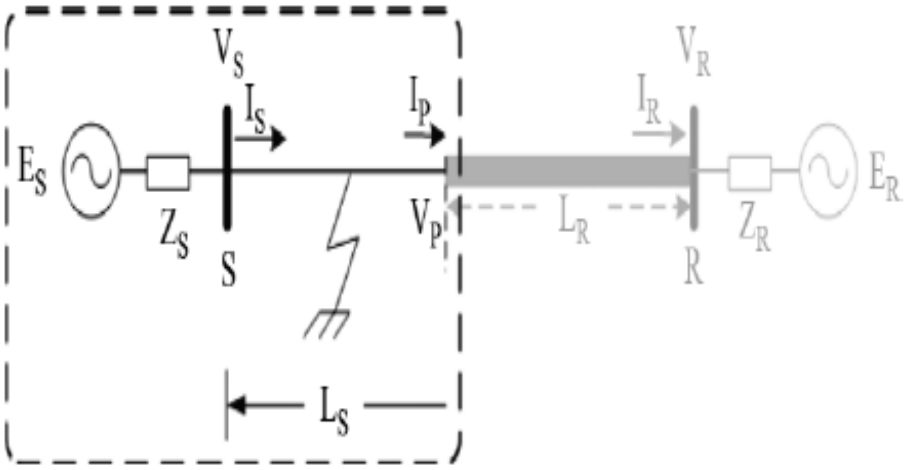

Fig.5. A fault on the overhead line section.

Where $Z_{C,S} = \sqrt{\frac{Z_S}{Y_S}}$ and $r_s = \sqrt{Z_S Y_S}$, in which and are respectively the positive sequence $r_R = \sqrt{Z_R Y_R}$ where $Z_R and\ Y_R$ are impedance and admittance of the underground power cable LR.MR and NR are given by

$\boldsymbol{M_R} = \frac{1}{2} (V_{P,S} + Z_{C\,R} I_{P,S})\, e^{-r_R} L_R - \frac{1}{2} (V_R + Z_{C,R} I_R)$.....3.13

$N_R = \frac{1}{2} (V_R - Z_{C\,R} I_R) - \frac{1}{2} (V_R + Z_{C,R} I_R)\, e^{r_R} L_R$ 3.14

Where $Z_{C,R} = \sqrt{\frac{Z_R}{Y_R}}$

Step 2: **Assume a fault on the left side of tap point P.** We assume that the fault occurs on the overhead line LS , as shown in Fig.3. 4. Given the healthy section of the cable LR, we can similarly derive the voltage and current phasors at P in terms of the receiving end data (VR, IR)

$\boldsymbol{V_{P,R}} = \frac{(V_R + Z_{C,R} I_R}{2}\, e^{r_R} L_R + \frac{(V_R - Z_{C,R} I_R)}{2}\, e^{-r_R} L_R$ 3.15

$I_{P,R} = \frac{1}{Z_{C,R}} [\frac{(V_R + Z_{C,R} I_R}{2}\, e^{r_R} L_R - \frac{(V_R - Z_{C,R} I_R)}{2}\, e^{-r_R} L_R]$ 3.16

Now we derive the fault location index, D2 using voltage and current phasors at tap point P and bus S and the line length LS . Substituting VP,R ,IP,R expressed in (15), (16) into , in (5) and equating (6) to the newly derived (5) with the characteristic impedance, ZC,S and the propagation constant, ΓS for the overhead line section, respectively, the fault location index D_2 can be obtained as follows:

$D_2 = \frac{In(\frac{N_S}{M_S})}{2r_S L_S}$……...…3.17

Where,

$\boldsymbol{M_S} = \frac{1}{2}(V_S + Z_{C,S}\, I_{S,})\, e^{-r_S L_S} - \frac{1}{2}(V_{P,R} + Z_{C,S}\, I_{P,R})$……3.18

$\boldsymbol{N_S} = \frac{1}{2}(V_{P,R} - Z_{C,S}\, I_{P,R,})\, - \frac{1}{2}(V_S + Z_{C,S}\, I_S)\, e^{r_S L_S}$……3.19

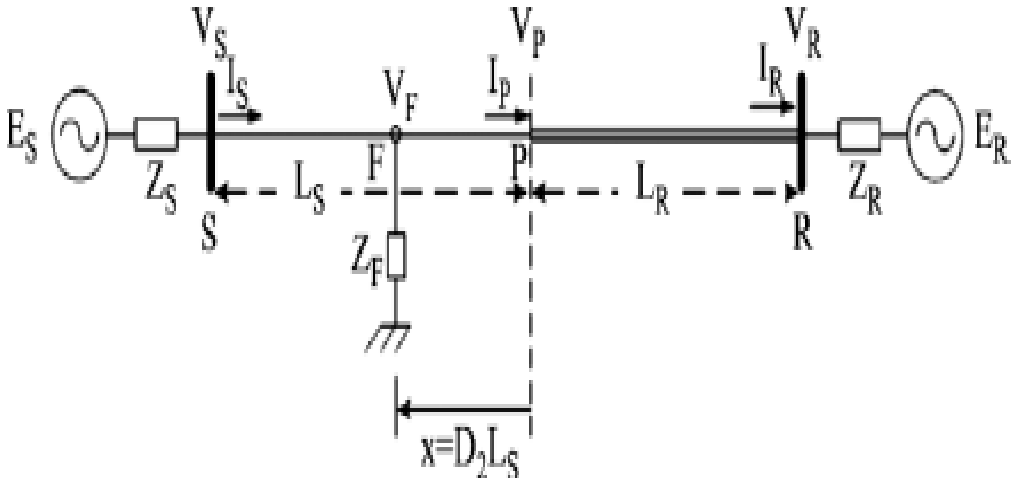

Fig.6. A fault occurs at a distance $x=D_2L_S$ away from tap point P.

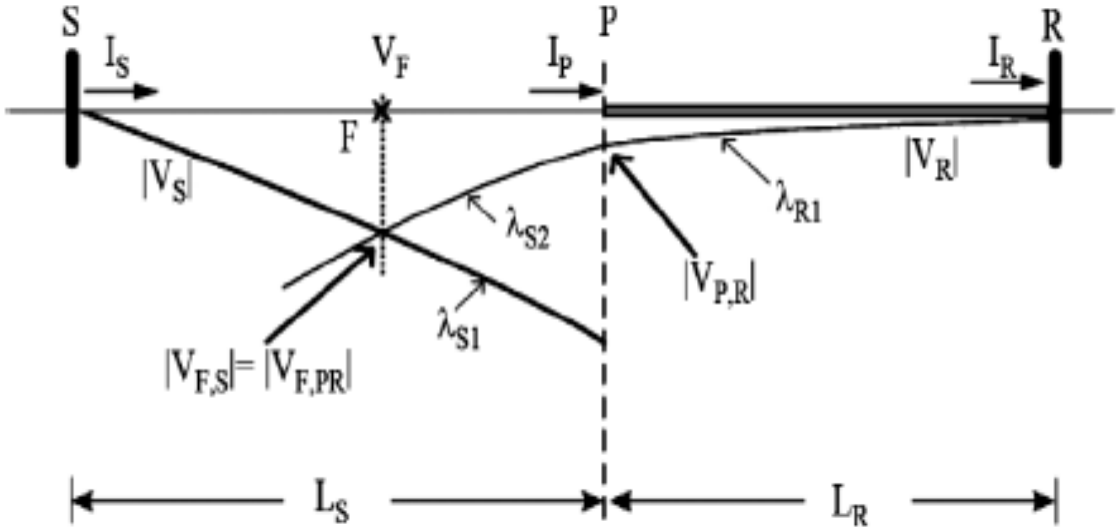

Fig.7: Relationship between the curves of |VS| and |VR| when calculating D_2.

Step 3: *Faulted section identification/fault location estimation.* Suppose that a fault occurs at the point with a distance of $x=D_2L_S$ km away from tap point P on the L_S section of a transmission line shown in Fig.3.5. We know that the voltage magnitudes and angles at the fault point F obtained from the quantities of two terminals are equal when using synchronized measurements. For ease of illustration, we only draw the two voltage magnitude profiles derived from buses S and R, as shown in Fig.3. 6. In Fig.3. 6, λS1 denotes the curve for the variation of |VS|;λR1 and λR2 denote the two parts of the curve for the variation of |VR| on the LR and LS sections, respectively. Note that the slopes of λR1 and λR2 are different because the line impedances of the LR and the LS sections are not uniform. Moreover, the curves of |VS| and |VR| are both almost linearly decreased from buses and orienting to the fault position (Benmouyal, 1995). As shown in Fig.3. 6, the intersection point of the curves

λS1 and λR2 pertains to the amplitude of the fault voltage VF. By using the relationship |VF,PR|=|VF,S| or VF,PR=VF,S as mentioned in *Step 2*, the index D2 can be obtained as shown in (17), where VF,PR and VF,S are derived from rewriting (3.5) and (3.6) as

$$\boldsymbol{V_{F,PR}} = \frac{(\boldsymbol{V_{P,R}} + \boldsymbol{Z_{C,S}}\boldsymbol{I_{P,R}})}{2}\, e^{\gamma s} D_2 L_R + \frac{(\boldsymbol{V_{P,R}} - \boldsymbol{Z_{C,S}}\boldsymbol{I_{P,R}})}{2}\, e^{-\gamma s} D_2 L_R \quad \text{.....3.20}$$

$$\boldsymbol{V_{F,PR}} = \frac{1}{2}\, e^{-\gamma s} L_S\, (V_S + Z_{C,S}\, I_S)\, e^{\gamma} D_2 L_R + \frac{1}{2} e^{\gamma s} L_S\, (V_S - Z_{C,S})\, e^{-\gamma s} D_2 L_S \quad \text{.....3.21}$$

Where $V_{P,R}$ and $I_{P,R}$ are expressed in (3.15) and (3.16), respectively. Since the index D2 , which is termed as the per-unit fault location index, is in reference with tap point P and the Ls is defined as reference per-unit length, the obtained value D2 is obviously in the interval [0,1].

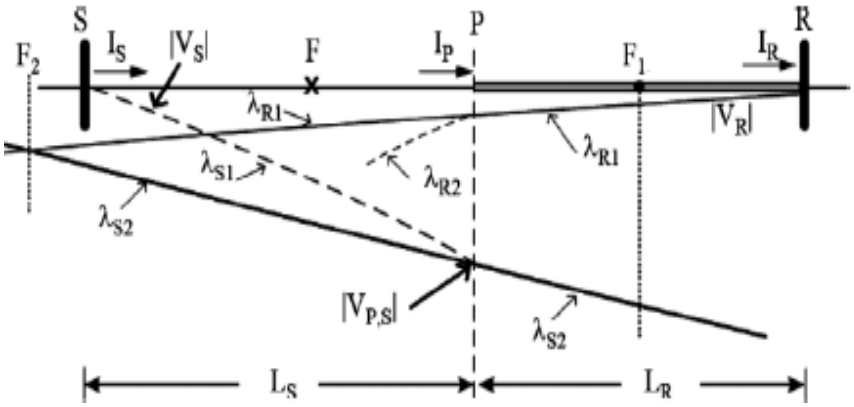

Fig. 8: Relationship between the curves of |Vs| and |VR| when calculating D1.

Meanwhile, the index D1 shown in (12) is obtained by assuming a fault on the right side (the cable section) of tap point P . The relationship between the curves of and for this case is illustrated in Fig.3. 7. Since the curves of |Vs| and |VR| are both decreased from buses S and R orienting to the correct fault position, in a similar manner, one can clearly observe that the curves λR1 and λS2 (with λS2 being part of the curve |VS| in the LR section) shown in Fig. 7 will not have any intersection points on the LR section. Instead, as the fault is assumed on the LR section, the slopes of curves λR1 and λS2 are thus extended to the LS section to calculate the index D1 as shown in Fig. 3.7. As a result, the curve λR1 will intersect with curve λS2 at the point F2. This fact indicates that the index D1 certainly converges on a value larger than 1 because the index D1 is with respect to bus R (as a reference) and the line length LR is defined as reference per-unit length. However, the derived fault point F2 is incorrect because the correct curves of |VR| and |VS| on the LS section are λR2 and λS1, respectively. Based on the foregoing discussions, we conclude that if the index D2 is in the interval[0,1] and the index D1 is larger than 1, one can identify that the fault occurs on the section of a two-section compound line, such as in Fig.3.5. In a similar manner, we can determine the relationships between the two indices,D1 and D2 , when dealing with a fault on the LR section or at tap point P . All the specific relationships between the two indices D1 and D2 from which one can identify the faulted line section/fault location are Summarized in Table I. Based on a similar process, we will develop a technique for the identification of the faulted section/fault location with general multi section compound lines in the next subsection.

1) *Two-Terminal N-Section(N>=2) Compound Lines:* In practice, the structure of compound transmission line systems is usually more complicated than the two-section case mentioned above. Now we move to more general multisection compound transmission line cases. Consider an N-section (N>=2) compound line depicted in Fig.3.8. PMUs or digital relays are installed at sending bus and receiving bus. Therefore, we can obtain the synchronized voltage

and current phasors at both terminals of the considered system. The length of every section is denoted as L1, L2,…, LN-1 and LN. *Every line* section may be composed by either an overhead line or an underground power cable. Two consecutive line sections may be either overhead lines, both underground cables, or an overhead line with an underground cable. For example, L1 and L2 in Fig.3.8 are both overhead lines, but their line impedances are very different (the conductor L1 of may be ACSR795D, while the conductor of may be ACSR636D)

The proposed fault location scheme for general two-terminal N-section compound transmission lines can be composed of two portions: *The N Fault Location Indices Derivation*: In order to illustrate the proposed fault location technique in a convenient manner, suppose first that a fault occurs at the point F, which is x km away from the receiving end R and L on the section of a transmission line shown in Fig.3.8. The line length L1 is defined as reference length of the derived fault location indices. The fault location scheme for the fault on the L3 section is divided into three procedures, as described below:

Procedure 1: Derive voltage/current phasors at point P3,R

As shown in Fig. 8, since the sections L1 and L2 are both healthy, the voltage and current at any point on the L1 or L2 can be derived by applying boundary conditions of bus R into (3) and (4) in terms of the line parameters of the L1 or L2 . As a result, the voltage and current phasors(VP3,R , IP3,R) at tap point P3,R can be derived using successive algebraic substitution steps from the data sets(VR, IR) at receiving end R. This is expressed in matrix form as follows:

$$\begin{bmatrix} V_{P3,R} \\ I_{P3,R} \end{bmatrix} = \boldsymbol{T_{R2}} \cdot \boldsymbol{T_{R1}} \cdot \begin{bmatrix} V_R \\ I_R \end{bmatrix} \quad \text{.....(3.22)}$$

where TR1 and TR2 are defined as the phasor transformation matrices of bus R and the subscripts 1 and 2 denote the use of the line parameters of the L1 and L2 sections, respectively. The general form of the matrix TR is given as the following:

$$T_{Rm} = \frac{1}{2}\begin{bmatrix} e^{\Gamma_{Lm}L_m} + e^{-\Gamma_{Lm}L_m} & Z_{C,Lm}\cdot(e^{\Gamma_{Lm}L_m} - e^{-\Gamma_{Lm}L_m}) \\ \frac{e^{\Gamma_{Lm}L_m} - e^{-\Gamma_{Lm}L_m}}{Z_{C,Lm}} & e^{\Gamma_{Lm}L_m} + e^{-\Gamma_{Lm}L_m} \end{bmatrix} = \begin{bmatrix} \cosh(\Gamma_{Lm}L_m) & Z_{C,Lm}\cdot\sinh(\Gamma_{Lm}L_m) \\ \frac{\sinh(\Gamma_{Lm}L_m)}{Z_{C,Lm}} & \cosh(\Gamma_{Lm}L_m) \end{bmatrix} \quad (\text{.....3. 23}$$

Where ZC,Lm and ΓLm are the positive sequence characteristic impedance and propagation constant for the Lm section, respectively.

Procedure 2: Derive voltage/current phasors at point Since the LN, LN-1,…,L5 and L4 are all healthy sections, we can likewise derive the voltage and current phasors (VP3,S, IP3,S) at tap point P3,S in Fig.3.8 via a series of substitutions from the data sets at sending end S using the following relations:

$$\begin{bmatrix} V_{P3,S} \\ I_{P3,S} \end{bmatrix} = T_{S4}\cdot T_{S5}\cdot\cdots\cdot T_{S(N-1)}\cdot T_{SN}\cdot\begin{bmatrix} V_S \\ I_S \end{bmatrix} \quad \text{……3.24}$$

where TS4,TS5,…,TS(N-1) and TSN are defined as the phasor transformation matrices of bus S . The general form of the matrix TS is shown below:

$$T_{Sm} = \frac{1}{2}\begin{bmatrix} e^{\Gamma_{Lm}L_m} + e^{-\Gamma_{Lm}L_m} & -Z_{C,Lm}\cdot(e^{\Gamma_{Lm}L_m} - e^{-\Gamma_{Lm}L_m} \\ \frac{-(e^{\Gamma_{Lm}L_m} - e^{-\Gamma_{Lm}L_m})}{Z_{C,Lm}} & e^{\Gamma_{Lm}L_m} + e^{-\Gamma_{Lm}L_m} \end{bmatrix}$$

$$= \begin{bmatrix} \cosh(\Gamma_{Lm}L_m) & -Z_{C,Lm}\cdot\sinh(\Gamma_{Lm}L_m) \\ \frac{-\sinh(\Gamma_{Lm}L_m)}{Z_{C,Lm}} & \cosh(\Gamma_{Lm}L_m) \end{bmatrix}. \quad (\text{.....3.25}$$

Procedure 3: fault location indices computation The application of the two-terminal fault location technique to solve for fault location x'=D_3L_3 away from the receiving end P3,R using two-terminal data sets (VP3,R, IP3,R) and (VP3,S, IP3,S) expressed in (22) and (24) is shown as follows:

$$D_3 = \frac{\ln\left(\frac{N_3}{M_3}\right)}{2\Gamma_{L3}L_3} \quad \text{.....3.26}$$

Where

$$M_3 = \frac{1}{2}(V_{P3,S} + Z_{C,L3}I_{P3,S})e^{-\Gamma_{L3}L_3} - \frac{1}{2}(V_{P3,R} + Z_{C,L3}I_{P3,R}) \quad \text{.....3.27}$$

$$N_3 = \frac{1}{2}(V_{P3,R} - Z_{C,L3}I_{P3,R}) - \frac{1}{2}(V_{P3,S} - Z_{C,L3}I_{P3,S})e^{\Gamma_{L3}L_3}. \quad \text{.....3.28}$$

Furthermore, we can normalizeD3 to obtain D3,R using the line length L1 as reference length, such that the fault location x=D3,RL1 away from bus R in the form

$$D_{3,R} = \frac{\ln\left(\frac{N_3}{M_3}\right)}{2\Gamma_{L3}L_1} + \alpha_3 \quad \text{.....3.29}$$

$$\alpha_3 = \frac{(L_1 + L_2)}{L_1}. \quad \text{.....3.30}$$

Using the principle of mathematical induction, the general form of fault location indices DK for all line sections can be obtained, where K=1…N are as follows:

$$D_K = \frac{\ln\left(\frac{N_K}{M_K}\right)}{2\Gamma_{LK}L_K} \quad \text{.....3.31}$$

and the general normalized fault location indices DK,R are written as the following:

$$D_{K,R} = \frac{\ln\left(\frac{N_K}{M_K}\right)}{2\Gamma_{LK}L_1} + \alpha_K \quad \text{.....3.32}$$

Where

$$M_K = \frac{1}{2}(V_{PK,S} + Z_{C,LK} I_{PK,S}) e^{-\Gamma_{LK} L_K} - \frac{1}{2}(V_{PK,R} + Z_{C,LK} I_{PK,R}) \quad \text{.....3.33}$$

$$N_K = \frac{1}{2}(V_{PK,R} - Z_{C,LK} I_{PK,R}) - \frac{1}{2}(V_{PK,S} - Z_{C,LK} I_{PK,S}) e^{\Gamma_{LK} L_K} \quad \text{.....3.34}$$

$$\alpha_K = \frac{\left(\sum_{n=1}^{K-1} L_n\right)}{L_1} \quad \text{.....3.35}$$

where the data sets (VPK,R, IPK,R) and (VPK,S, IPK,S) expressed in (3.33) and (3.34) can be derived in terms of the data sets (VR,IR) and (VS,IS) by rewriting (3.22) and (3.24) into general forms, as shown in the following:

$$\begin{bmatrix} V_{PK,R} \\ I_{PK,R} \end{bmatrix} = \left(\prod_{m=1}^{K-1} T_{R(K-m)}\right) \cdot \begin{bmatrix} V_R \\ I_R \end{bmatrix} \quad \text{.....3.36}$$

$$\begin{bmatrix} V_{PK,S} \\ I_{PK,S} \end{bmatrix} = \left(\prod_{m=K+1}^{N} T_{Sm}\right) \cdot \begin{bmatrix} V_S \\ I_S \end{bmatrix}. \quad \text{.....3.37}$$

Equations (3.36) and (3.37) are named as the measured-data converting equations for the two-terminal multi-section compound transmission lines. The Proposed Fault Section/ Fault Location Identification: So far, we have derived N fault location indices, DK and N normalized fault location indices. Now the problem is which fault location index set (DK,DK,R) is the correct set for accurately locating a fault. Theoretically, only one correct index set corresponds to a single fault. We propose an efficient searching algorithm for this purpose. The flowchart of the algorithm illustrates the operations of fault section/location identification strategies for two-terminal multi-section compound transmission lines. The details of the algorithm are explained in the following three steps: Step 1) As mentioned above, bus R and the line length L1 are selected as the receiving end and reference length. Base on the assumption that a midway fault occurs At y km away from bus R in section K, so y=DK,RL1.

Step 2) Generate the N Fault Location Index Set The data sets (VPK,R, IPK,R) and (VPK,S, IPK,S) can be derived by (36) and (37). Equations (31) and (32) are then applied to obtain the fault location index DK and DK,R, where K is from 1 to N . Step 3) Searching for correct fault location index set Similar to the results of two-section compound lines shown in Table I, we further propose three strategies for the efficient search for the correct fault location index set

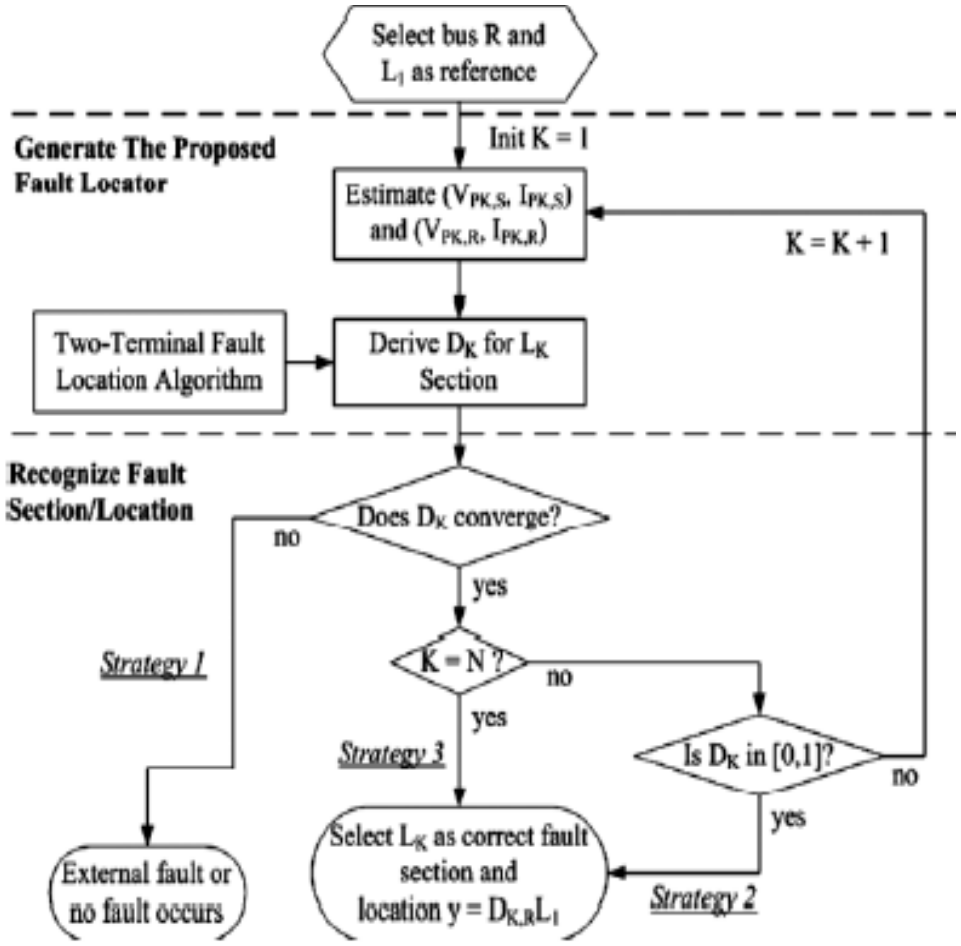

Fig.9. The proposed fault section selector/locator for two-terminal N-section compound lines.

Strategy 1: If DK any is an indefinite value, then an external fault or no fault occurs.
Strategy 2: From K=1 to N-1 , if the obtained DK falls within the interval [0,1], according to the two-terminal fault location theorem (Liu et al., 2008) then DK the is recognized as the correct fault location index and the correct fault distance y is DK,RL1 away from the receiving end R .
Strategy 3: Given K=N, since LN is the last line section of the proposed fault-locating procedures, it obviously indicates the fact that DN is identified as the correct fault location index and the correct fault distance y is DN,RL1 away from the receiving end R.

III. PERFORMANCE EVALUATION

A. Simulated Cases Evaluations

A Taipower 161 kV, transposed double-circuit four-section compound transmission line with zero sequence mutual coupling was simulated using the distributed parameter model. The double-circuit line can be treated as two independent single-circuit lines as only positive sequence data is used in the proposed scheme. Therefore, the double-circuit line model shown in Fig. 10 was intentionally established to test the performance of the proposed fault location algorithm. Line S-T is used to evaluate the performance of the proposed scheme for external faults. The simulated system was developed using MATLAB/SIMULINK® simulator (Math Works, 2002) with the use of 161 kV Transmission line parameters. All the measurements are filtered using the second-order Butterworth anti-aliasing filters with cutoff

frequency of 360 Hz. The sampling frequency is 1920 Hz (32 sampling points per cycle). A digital mimic filter and full-cycle DFT are employed to reduce decaying dc offset and to obtain the fundamental phasors.

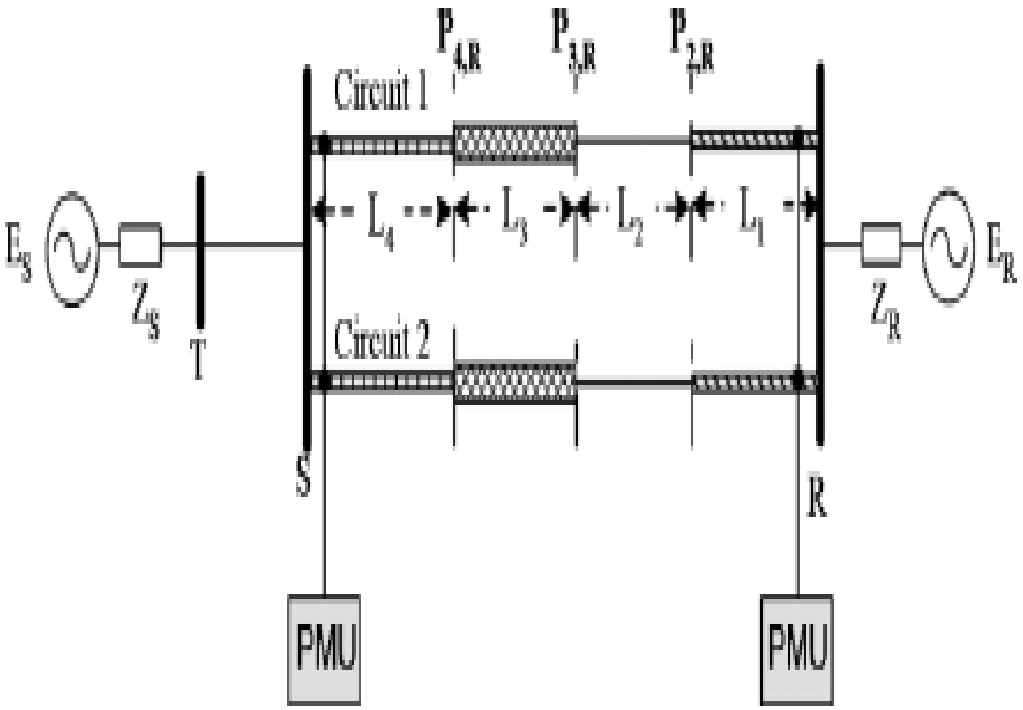

Fig. 10 . The simulation system consists of a transposed double-circuit four section compound transmission line and an external line S-T. The simulations have been conducted in reference to various system operations and fault conditions.

4. RESULTS AND DISCUSSION

In this research, the Matlab simulator is adopted to evaluate the performance of the proposed scheme. Fig. 4.1 depicts the response of the simulated system.

To demonstrate the robustness of the protection scheme, the simulations are conducted with respect to various system and fault conditions. In figure 4.2, fault inception time, fault-detection time, and tripping decision time, are shown respectively.

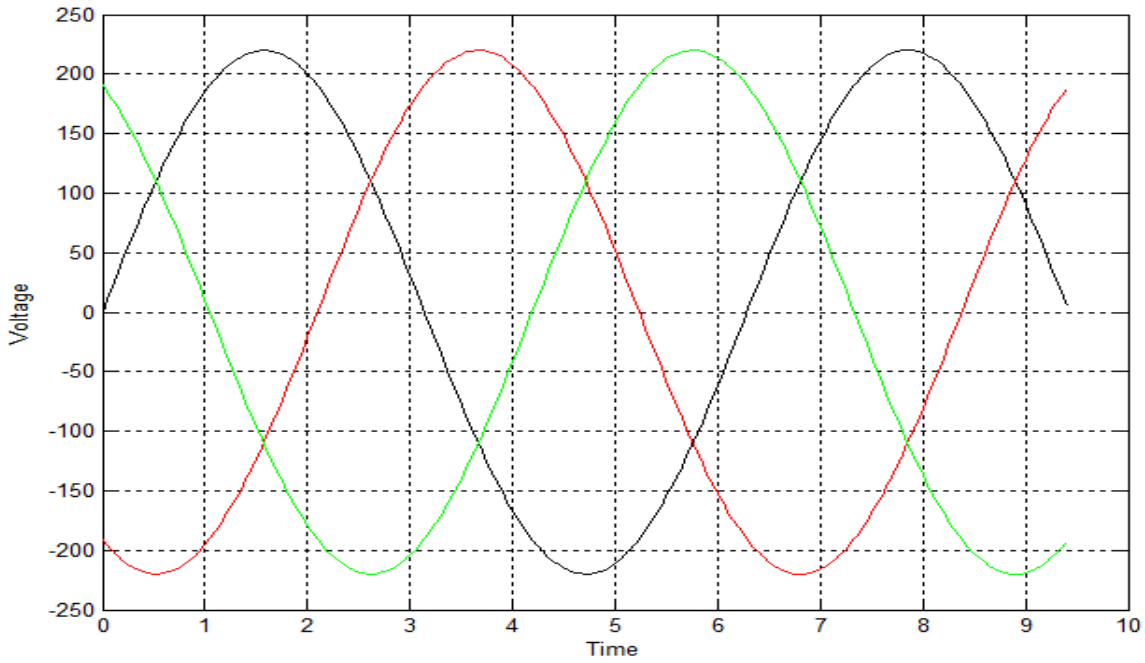

Fig.11: The response of the simulated system

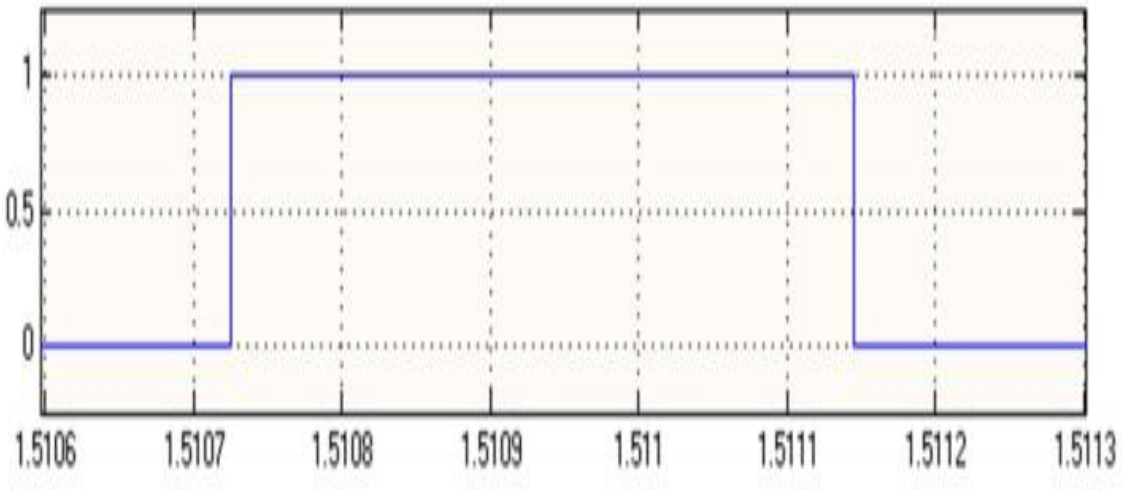

Fig. 12.: Fault inception time

4.1 DISCUSSION

The fault-on response curves of the proposed fault location indices DK(K=1-4) for a phase ab to ground fault (ab–g fault) on the line S-T (external fault) is shown in Fig. 4.1. The fault position is set at 6.6 km away from bus S , the fault resistance is 1 Ohm and the fault inception angle is zero degree with respect to phase- "ab" voltage waveform at bus S. Fig. 4.1 obviously shows that all of the indices do not converge. It also shows the fault-on response curves of the proposed fault location indices for a phase "ab" to ground fault (a–g fault) on the L4 (internal fault). The fault position is set at 2.712 km (80% of the length L4) away from, P4,R, the fault resistance is 10 Ohm and the fault inception angle is zero degree with respect to phase- "ab" voltage at bus . In Fig. 4.2, the time taken to reach the threshold voltage is about 1.510760 ms. While the time taken to reach the threshold angle is also 1.511109 ms, then the fault can be detected in about 0.000349 ms. A single phase to ground fault is located on transmission line TL3,

5. CONCLUSION

The positional protection using GPS is a high speed protection system and offers a high accuracy in fault location. The protection system monitors the network to which it is connected and is not limited to individual unit plant as in traditional protection scheme.

The proposed scheme only uses a composite index to achieve high-speed relaying tasks including fault detection, direction discrimination, and classification. The scheme also provides accurate fault location.

Extensive simulation studies demonstrate that the complete protection scheme is not significantly affected by various system situations, fault events, and line configurations. The tripping decision time of the scheme is very fast and stable, whose value on average is well within half a cycle.

REFERENCES

A.O Balogun: Impact Sector Reforms on Nigeria Electricity, Conference proceedings of the International Conference and Exhibition in Power Systems, Nigeria, July 2007, pp 123-128.

A. A. Girgis, D. G. Hart, and W. L. Peterson, ―A new fault location technique for two and three-terminal lines,‖ *IEEE Trans. Power Del.*, vol. 7, no. 1, pp. 98–107, Jan. 1992.

A. L. Dalcastagnê, S. N. Filho, H. H. Zürn, and R. Seara, ―An iterative two-terminal fault locationmethod based on unsynchronized phasors,‖ *IEEE Trans. Power Del.*, vol. 23, no. 4, pp. 2318–2329, Oct. 2008.

A.G. Phadke and J. S. Thorp, *Synchronized Phasor Measurements and Their Applications*. Berlin, Germany: Springer, 2008.

Power System Blockset User's Guide The Math Works, Inc, 2002.

C. A. Gross, *Power System Analysis*. New York: Wiley, 1986.

C. W. Liu, Applied protective relaying,‖ Relay-Instrument Division, Westinghouse Electric Corp., Coral Springs, FL, 1982.

C. J. Lee, J. B. Park, J. R. Shin, and Z. M. Radojevié, ―A new two-terminal numerical algorithm for fault location, distance protection, and arcing fault recognition,‖ *IEEE Trans. Power Syst.*, vol. 21, no. 3, pp.1460–1462, Aug. 2006. Y. H. Lin, C. W. Liu, and C. S. Chen, ―An adaptive PMU based fault detection/location technique for transmission lines with consideration of arcing fault discrimination part I : Theory and algorithms,‖ *IEEE Trans. Power Del.*, vol. 19, no. 4, pp. 1587–1593, Oct. 2004.

C. W. Liu, K. P. Lien, C. S. Chen, and J. A. Jiang, ―A universal fault location technique for N-terminal transmission lines,‖ *IEEE Trans. Power Del.*, vol. 23, no. 3, pp. 1366 1373, Jul. 2008.

C. S. Chen, C. W. Liu, and J. A. Jiang, ―A new adaptive PMU based protection scheme for transposed/untransposed parallel transmission lines,‖ *IEEE Trans. Power Del.*, vol. 17, no. 2, pp. 395–404, Apr. 2002.

C. S. Yu, ―An unsynchronized measurements correction method for two-terminal fault location problems,‖ *IEEE Trans. Power Del.*, vol. 25, no. 3, pp. 1325–1333, Jul. 2010.

D. Novosel, D. G. Hart, E. Udren, and M. M. Saha, ―Fault locationusing digital relay data,‖ *IEEE Comput. Appl. Power*, vol. 8, no. 3, pp.45–50, Jul. 1995.

G. Benmouyal, ―Removal of DC-offset in current waveforms using digital mimic filtering,‖ *IEEE Trans. Power Del.*, vol. 10, no. 2, pp. 624–630, Apr. 1995.

J. Izykowski, E. Rosolowski, P. Balcerek,M. Fulczyk, andM.M. Saha,―Accurate noniterative fault location algorithm utilizing two-end unsynchronizedmeasurements,‖ *IEEE Trans. Power Del.*, vol. 25, no. 1,pp. 72–80, Jan. 2010.

M. Kezunovic, J. Mrkic, and B. Perunicic, ―An accurate fault locationalgorithm using synchronized sampling,‖ *Elect. Power Syst. Res. J.*,vol. 29, no. 3, pp. 161–169, May

1994.

M. Kezunovic and B. Perunicic, ―Automated transmission line fault analysis using synchronized sampling at two ends,‖ *IEEE Trans. Power Syst.*, vol. 11, no. 1, pp. 441 447, Feb. 1996.

M. Gilany, E. S. T. Eldin, M. M. A. Aziz, and D. K. Ibrahim, ―An accurate scheme for fault location in combined overhead line with underground power cable,‖ in *Proc. IEEE Power Eng. Soc. Gen. Meet.*, San Francisco, CA, Jun. 12–16, 2005, vol. 3, pp. 2521 2527.

S. M. Brahma, ―Fault location scheme for a multi-terminal transmissionline using synchronized voltage measurements,‖ *IEEE Trans.Power Del.*, vol. 20, no. 2, pp. 1325–1331, Apr. 2005.

T. Takagi, Y. Yamakoshi, J. Baba, K. Uemura, and T. Sakaguchi, ―Anew algorithm of an accurate fault location for EHV/UHV transmissionlines: Part I—Fourier transformationmethod,‖ *IEEE Trans. PowerApp. Syst.*, vol. PAS-100, no. 3, pp. 1316 1323, Mar. 1981.

T. Takagi, Y. Yamakoshi, M. Yamaura, R. Kondow, and T. Matsushima,―Development of a new type fault locator using theone-terminal voltage and current data,‖ *IEEE Trans. Power App. Syst.*,vol. PAS-101, no. 8, pp. 2892–2898, Aug. 1982.

X. Yang, M. S. Choi, S. J. Lee, C. W. Ten, and S. I. Lim, ―Fault location for underground power cable using distributed parameter approach,‖ *IEEE Trans. Power Syst.*, vol. 23, no. 4, pp. 1809–1816, Nov. 2008.

Y. Liao andM. Kezunovic, ―Optimal estimate of transmission line fault location considering measurement errors,‖ *IEEE Trans. Power Del.*,vol. 22, no. 3, pp. 1335–1341, Jul. 2007.